FORCED OSCILLATION OF SIMPLY-SUPPORTED MICROBEAMS CONSIDERING NONLINEAR EFFECTS

Rafiee[1], M., Nezamabadi[2], A.

[1] Mechanical Engineering Department, Islamic Azad University ,Arak Branch, Young Rsearchers Club, Arak, Iran.
[2] Mechanical Engineering Department, Islamic Azad University ,Arak Branch, Arak, Iran.

Received Date: 01 September 2010; Accepted Date: 16 October 2010

Abstract

Nonlinear free and forced oscillation of microscale simply supported beams is investigated in this paper. Introducing a material length scale parameter, the nonlinear model is conducted within the context of non-classical continuum mechanics. By using a combination of the modified couple stress theory and Hamilton's principle the nonlinear equation of motion is derived. The nonlinear frequencies of a beam with initial lateral displacement are discussed. Equations have been solved using an exact method for free vibration and multiple times scales (MTS) method for forced vibration and some analytical relations have been obtained for natural frequency of oscillations. The results have been compared with previous work and good agreement has been obtained. Also forced vibrations of system in primary resonance have been studied and the effects of different parameters on the frequency-response have been investigated. It is shown that the size effect is significant when the ratio of characteristic thickness to internal material length scale parameter is approximately equal to one, but is diminishing with the increase of the ratio. Our results also indicate that the nonlinearity has a great effect on the vibration behavior of microscale beams.

Keywords: Microbeam, Free and forced vibration, nonlinear vibration

1. INTRODUCTION

Thin beams have been widely used in micro- and nano-scale devices and systems such as sensors, actuators, microscopes, MEMS and NEMS [1–4] for applications ranging from sensing and communications to energy harvesting, fundamental studies of quantum mechanical systems, etc. Across these applications, the characteristic thicknesses of the beams are typically on the order of microns or even sub-microns. As reported in many papers (e.g., [5–8]), the microscale beams may be made of metals, polymer, traditional silicon-based materials or functionally graded materials (FGMs). The design of microbeams is dominated by several basic requirements. One of these basic requirements is to attain mechanical and vibration properties to match the required functionality of interest. It is not surprising, therefore, that the literature on this topic is constantly expanding. The classical continuum mechanics theories are not capable of prediction and explanation of the size-dependent behaviors which occur in micron- and sub-micron-scale structures. However, nonclassical continuum theories such as higher-order gradient theories and the couple stress theory are acceptably able to interpret the size-dependencies. In the current work, however, theoretical analysis will not be conducted within the context of classical continuum mechanics. Though the classical continuum models are relevant to some extent, the length scales associated with material's microstructure (such as lattice spacing between individual atoms) are often sufficiently small to call the applicability of classical continuum models into question [10]. Indeed, the size dependence of material deformation behavior in micronscale has been observed experimentally in the last two decades. Related work on this topic appears to have started in the 1990s. Some of the key contributions in this area were made by Fleck et al. [11], Ma and Clarke [12], Stolken and Evans [13], Chong and Lam [14], Lam et al. [15], and

[1] Corresponding Author, Email: mrafiee20@gmail.com

McFarland and Colton [16]. The size dependence phenomenon has been observed in the materials of either metals or polymers. In these experimental works, the microscale structures studied may be copper wires, silver single crystal, nickel beams, or epoxy polymeric beams. These experimental results certainly demonstrate that the size dependence is intrinsic to certain materials with microstructures. In 1960s some researchers introduced the couple stress elasticity theory [17–19]. In the constitutive equation of this theory, two higher-order material length scale parameters appear in addition to the two classical Lame constants. As recent applications of the couple stress theory, here two works are described. Zhou and Li [27] employed this theory to investigate the static and dynamic behavior of a micro-bar in torsional loading. Kang and Xi [28] studied the resonant frequencies of a micro-beam and indicated that these frequencies are size-dependent.

Recently, Yang et al. [20] proposed a modified couple stress theory, in which the constitutive equations contain only one single additional internal material length scale parameter besides two classical material constants. Owing its advantageous expression, the modified couple stress (non-classical) theory has attracted many researchers in the past years. As an example, Park and Gao [7] have studied the statically mechanical properties of Bernoulli–Euler cantilever beams by using this non-classical elasticity theory. The corresponding results were applied to explain bending test of epoxy polymeric beams successfully. This modified couple stress theory has also been used to study the dynamic properties (e.g., natural frequencies) of Euler–Bernoulli microbeams by Kong et al. [21]. In their study, two boundary value problems (one for simply supported beam and another for cantilevered beam) were solved and size effect on the natural frequencies for these two kinds of boundary conditions were evaluated. It was found that the natural frequencies of the mircobeams predicted by the modified couple stress theory are generally higher than those predicted by the classical Euler–Bernoulli beam theory. The objective of the present paper is to establish a nonlinear non-classical Euler–Bernoulli beam model for microscale beams by using the modified couple stress theory. The beam material is assumed to obey the modified couple stress theory, as developed by Yang et al. [20]. This new nonlinear model contains a material length scale parameter and can capture the size effect. The nonlinear equation of motion will be derived by using the Hamilton's principle. The nonlinear term added, assumed supported between two axially immobile supports. Based on the equation of motion derived, the free vibration of pinned–pinned microbeams will be studied. It will be shown that the effect of material length scale parameter and nonlinearity on the vibration frequencies are significant. The difference between the nonlinear non-classical results and the linear results (both classical and non-classical) will be quantitatively shown and analyzed.

2. FORMULATION

The system under consideration is a microscale simply supported beam of length L, mass density ρ, cross-section height h and cross-section width b. The cross-section of the beam is symmetric (either rectangular or circular). We will consider the nonlinear vibrations of microbeams with transverse dimensions ranging from several micro-meters to hundreds of micro-meters.

The linear equation of motion based on a modified couple stress elasticity theory is given by [21]

$$\left(EI + GA\ell^2\right)\frac{\partial^4 w}{\partial x^4} + \frac{\partial^2 w}{\partial t^2} = q(x,t) \qquad (1)$$

where E is the Young's modulus of elasticity, I is the moment of inertia of the cross-section, A is the cross-sectional area, G is a Lame's constant ($G = E/[2(1 + \mu)]$ is also known as the shear modulus, where μ is Poisson's ratio), ℓ is a material length scale parameter, $q(x,t)$ is a transverse loading, and $w(x, t)$ is the lateral deflection of the beam; x and t are the axial coordinate and time, respectively. Since the derivation of Eq. (1) is based on a refined Euler–Bernoulli beam theory, the corresponding theoretical model described is called ''non-classical Euler–Bernoulli beam model". It is immediately found that the above equation has introduced a material length scale parameter ℓ, which represents the microstructure-dependent effect.

As reported by Sadeghian et al. [22], the choice of appropriate structural analysis model of the microscale beam depends on the magnitude of the lateral deflection compared to the thickness of the beam. The theoretical model described in Eq. (1) may be an adequate representation for the case that the deflection is considerably small (e.g., the deflection is smaller than the thickness of the microbeam). For the case that the deflection is relatively large (e.g., the deflection is approximately equal to or larger than the thickness of the microbeam), bending-stretching coupling terms need to be taken into account, since the effects of nonlinearity on the mechanical and vibration properties become observable. The nonlinear equation of motion of a microbeam with immovable ends will be formulated by using the Hamilton's principle. According to the modified couple stress theory [34], the bending strain energy U_m of the microbeam is a function of both the strain (conjugated with stress) and the curvature (conjugated with couple stress). Then the bending strain energy in a deformed microbeam is given by [7]

$$U_m = -\frac{1}{2}\int_0^L M_x \frac{\partial^2 w}{\partial x^2} dx - \frac{1}{2}\int_0^L \gamma_{xy} \frac{\partial^2 w}{\partial x^2} dx \tag{2}$$

where the resultant moment M_x and the couple moment Y_{xy} are defined, respectively, by

$$M_x = \int_A \sigma_{xx} z dA \tag{3}$$

$$Y_{xy} = \int_A m_{xy} dA \tag{4}$$

In the above two equations, σ_{xx} and m_{xy} are, respectively, defined by

$$\sigma_{xx} = -Ez \frac{\partial^2 w}{\partial x^2} \tag{5}$$

$$m_{xy} = -G\ell^2 \frac{\partial^2 w}{\partial x^2} \tag{6}$$

Then U_m may be rewritten as

$$U_m = \frac{1}{2}\int_0^L \left(EI + GA\ell^2\right)\left(\frac{\partial^2 w}{\partial x^2}\right)^2 dx \tag{7}$$

By neglecting the body force and body couple, the work done by the externally transverse loading $q(x, t)$ may be written as

$$W = \int_0^L q(x,t) w(x) dx \tag{8}$$

The kinetic energy of the microbeam is given by

$$K = \frac{1}{2}\int_0^L \rho A \left(\frac{\partial w}{\partial t}\right)^2 dx = \frac{m}{2}\int_0^L \left(\frac{\partial w}{\partial t}\right)^2 dx \tag{9}$$

in which $m = \rho A$ is the beam mass of per unit length. According to the Hamilton's principle, the dynamic equation of motion of this beam as well as all possible boundary conditions can be derived by using the following variational equation

$$\delta \int_{t_1}^{t_2} \left(K - U_m - W\right) dt = 0 \tag{10}$$

Substituting Eqs. (7)–(9) into Eq. (10), one obtains

$$\begin{aligned}&\int_{t_1}^{t_2}\int_0^L \{-\left(EI + GA\ell^2\right)\frac{\partial^4 w}{\partial x^4} - m\frac{\partial^2 w}{\partial t^2} + q - \int_{t_1}^{t_2}\left[\left(EI + GA\ell^2\right)\frac{\partial^3 w}{\partial x^3}\delta w\right]_0^L dt \\ &-\int_{t_1}^{t_2}\left[\left(EI + GA\ell^2\right)\frac{\partial^2 w}{\partial x^2}\delta w'\right]_0^L dt + \int_0^L \left[\frac{\partial w}{\partial t}\delta w\right]_{t_1}^{t_2} dx = 0\end{aligned} \tag{11}$$

In view of Eq. (11), the nonlinear equation of motion of the beam in terms of $w(x, t)$ is given by

$$\left(EI + GA\ell^2\right)\frac{\partial^4 w}{\partial x^4} + m\frac{\partial^2 w}{\partial t^2} = q(x,t) \tag{12}$$

and the boundary conditions are

$$\frac{\partial^3 w}{\partial x^3} = 0 \text{ or } w = 0 \text{ at } x = 0 \text{ and } x = L, \tag{13a}$$

$$\frac{\partial^2 w}{\partial x^2} = 0 \text{ or } \frac{\partial w}{\partial x} = 0 \text{ at } x = 0 \text{ and } x = L. \tag{13b}$$

It can be seen from Eq. (12) that the deflections of the beam are related to two types of material parameters: one associated with ρA, EA and EI as in classical beam model and the other associated with $GA\ell^2$. Therefore, the current refined Euler–Bernoulli beam model based on the modified couple stress elasticity theory contains one additional internal material constant besides three classical material parameters. As can be expected, the presence of ℓ enables us to analyze the size effect. Defining the following quantities

$$\xi = x/L, \quad \eta = w/L, \quad \tau = \left[\frac{EI}{\beta m L^4}\right]^{1/2} t$$

$$\alpha = L/r, \quad r = \sqrt{I/A}, \quad \beta = \frac{1}{1+\left[6/(1+\mu)\right]\times(\ell/h)^2}$$

$$\Gamma = \frac{T_0 L^2}{EI + GA\ell^2} = \beta\frac{T_0 L^2}{EI} = \beta\Gamma_L, \tag{14}$$

$$\phi = \frac{qL^3}{\left(EI + GA\ell^2\right)} = \beta\frac{qL^3}{EI},$$

$$\kappa = \frac{EAL^2}{2\left(EI + GA\ell^2\right)} = \frac{\beta}{2}\alpha^2$$

Eq. (12) may be written in the dimensionless form

$$\frac{\partial^4\eta}{\partial\xi^4} + \left[\Gamma - \kappa\int_0^1\left(\frac{\partial\eta}{\partial\xi}\right)^2 d\xi\right]\frac{\partial^2\eta}{\partial\xi^2} + \frac{\partial^2\eta}{\partial\tau^2} = \phi \tag{15}$$

Since Eq. (15) is represented in a dimensionless form, the current non-classical beam model may be used to analyze the dynamic responses of microbeams, regardless of the beam materials or length scales. It may be also mentioned that the equation of motion, (15), is essentially based on the Euler–Bernoulli beam assumptions. Like all other analytical models, therefore, the newly developed beam model has limitations, which are contingent upon the applicability of the modified couple stress theory. Specifically, the microbeam must be slender so that the Euler–Bernoulli beam assumptions are applicable. For microbeam with relatively large width (b), however, the current Euler–Bernoulli beam theory may be inadequate for predicting the response of microbeams.

In this paper, the microbeam under consideration is assumed to be pinned–pinned. For such a beam system, the deflection and moment are zero at both ends. Then the boundary conditions can be written in the dimensionless form

$$\eta = 0 \quad \text{and} \quad \frac{\partial^2\eta}{\partial\xi^2} = 0 \quad \text{at} \quad \xi = 0,1 \tag{16}$$

Before closing this section, it should be mentioned that, for analysis convenience, the beam material is chosen to be epoxy. Thus, the material constants used here are E = 1.44 GPa and $\ell = 1.76\ \mu$m [7]. In the following analysis, for comparison purpose, we will choose a = 30 and two different values of Poisson's ratio (i.e., μ = 0 and μ = 0.38).

3. FREE VIBRATION

In this section, the free vibration of a microscale beam with both ends immoveable will be analyzed. It is assumed that the external transverse force $q(x,t)$ is absent. Based on this assumption, Eq. (15) becomes

$$\frac{\partial^4\eta}{\partial\xi^4} - \left[\kappa\int_0^L\left(\frac{\partial\eta}{\partial\xi}\right)^2 d\xi\right]\frac{\partial^2\eta}{\partial\xi^2} + \frac{\partial^2\eta}{\partial\tau^2} = 0 \tag{17}$$

As already mentioned in the foregoing, the nonlinearity is caused by the immoveable ends which are not allowed to move to any appreciable extent relative to the initial coordinates of the beam ends. Therefore, the axial inertia may be also neglected. The initial conditions considered in the current work are:

$$w(L/2,0) = w_{\max}, \quad \frac{\partial w(L/2,0)}{\partial t} = 0 \tag{18}$$

The dimensionless initial conditions given by Eq. (18) become

$$\eta(1/2,0) = w_{\max}, \quad \frac{\partial w\ (1/2,0)}{\partial t} = 0 \tag{19}$$

Assume that

$$\eta(\xi,\tau) = \psi(\xi)\,q(\tau) \tag{20}$$

where $\psi(\xi)$ is the characteristic mode of a pinned–pinned beam and

$$\psi(\xi) = \sin(n\pi\xi) \quad n = 1,2,3,\ldots \tag{21}$$

The substitution of Eq. (20) into Eq. (17) leads to

$$\ddot{q} + \frac{\left(EI + GA\ell^2\right)(n\pi)^4}{mL^4\omega^2}q + \frac{EA(n\pi)^4}{4mL^2\omega^2}q^3 = 0 \tag{22}$$

where $(\ )^{\cdot} = \partial(\ )/\partial\hat{t}$ and $\hat{t} = \omega t$.

$$\omega = \left[\frac{\left(EI + GA\ell^2\right)(n\pi)^4}{mL^4}\right]^{1/2} \tag{23}$$

one obtains

$$\ddot{q} + q + \gamma q^3 = 0 \tag{24}$$

in which the dimensionless parameter γ is given by

$$\gamma = \frac{3L^2}{h^2\left\{1 + \left[6/(1+\mu)\right]\times\left(\ell/h\right)^2\right\}} \tag{25}$$

It is worth noting that Eq. (24) is a classical Duffing-type equation which represents a nonlinear oscillator without damping. This equation may be solved via various methods, such as the method of harmonic balance, equivalent linearization, generalized averaging and multiple scales method [24]. By multiplying (24) by $\dot{q}$ and integrating with respect to time, the following energy balance equation is obtained

$$\dot{q}^2 + q^2 + \frac{1}{2}\gamma q^4 = H = \text{constant.} \tag{26}$$

The constant H is evaluated from initial conditions. By assuming initial conditions (19), one has

$$H = w_{\max}^2 + \frac{1}{2}\gamma w_{\max}^4 \tag{27}$$

Putting H into (26) leads to

$$\dot{q}^2 = \left(w_{\max}^2 - q^2\right) + \frac{1}{2}\gamma\left(w_{\max}^4 - q^4\right) \tag{28}$$

By introducing new parameters χ_1 and χ_2 in the following way

$$\chi_1^2 = 1 + \gamma, \quad \chi_2^2 = \frac{\gamma}{2\chi_1^2} \tag{29a,b}$$

Such that the differential equation has solutions in terms of Jacobi elliptic function. Hence, Eq. (28) can be rewritten as follows:

$$\begin{aligned} \dot{q}^2 &= w_{\max}^2 - q^2 + \frac{\gamma}{2} w_{\max}^4 - \frac{\gamma}{2} q^4 \\ &= (\chi_1^2 - 2\chi_2^2\chi_1^2)(w_{\max}^2 - q^2) + \chi_1^2\chi_2^2(w_{\max}^4 - q^4) \\ &= (w_{\max}^2 - q^2)(\chi_1^2 - 2\chi_2^2\chi_1^2 + \chi_1^2\chi_2^2(w_{\max}^2 + q^2)) \\ &= (w_{\max}^2 - q^2)(1 + \chi_1^2\chi_2^2(w_{\max}^2 + q^2)) \end{aligned} \tag{30}$$

and it reduces to

$$\left(\frac{dq}{dK}\right)^2 = \left(w_{\max}^2 - q^2\right)\left(\chi_2^2 q^2 - \chi_2^2 + w_{\max}^2\right). \tag{31}$$

Then, assuming $q = \cos\varphi$ we can obtain Jacobi elliptic function [26] with the modulus k, defined by Eq. (29b),

$$K = \int_0^{\varphi} \frac{d\varphi}{\sqrt{1 - \chi_2^2 \sin^2\varphi}} \tag{32}$$

From the inversion of Eq. (31), the solution for q can be obtaion as follows:

$$q = cn[K,k] \tag{33}$$

The period of the function cn[K,k] is 4K and is defined by using the complete elliptic integral,

$$4K = 4\int_0^{\pi/2} \frac{d\varphi}{\sqrt{1-\chi_2^2 \sin^2 \varphi}} \tag{34}$$

Then, the corresponding frequency for this nonlinear problem for each mode is defined by using the following equation:

$$\omega_{nl} = \frac{\pi\sqrt{1+w_{\max}^2\gamma}}{2K} \tag{35}$$

4. FORCED VIBRATIONS

In this section, forced vibrations of the system will be considered. It is also considered that the excitation appears as an inhomogeneous term in the equations of motion [24] .
Let the system is exerted an external harmonic excitation $E(t)$ as:

$$E(t) = K\cos\Omega t \tag{36}$$

Equation (24) in the forced vibration case can be written as:

$$\ddot{q} + q + \gamma q^3 = K\cos\Omega t \tag{37}$$

Two types of excitations, primary resonances and non-resonant hard excitations will be discussed here and the frequency response equations and effects of some parameters will be investigated.

4.1. Primary resonances

In this case, it is supposed that the frequency of excitation **Ω** and linear frequency of the system ω_0 are near together as $\Omega \approx \omega_0$. So a detuning parameter σ is used to show the nearness of **Ω** to ω_0 as:

$$\Omega = \omega_0 + \varepsilon\sigma \tag{38}$$

Because there are no types of damping in the system, in linear state it is expected that when σ approaches to zero, system shows an unlimited oscillation, but in nonlinear state oscillations is limited by nonlinearities. As discussed later, to obtain a uniformly valid approximate solution the excitation must be in same order of the non-linear terms. So, in Eq. (36) it must be considered $K = \varepsilon k$. An approximate solution of the problem can be obtained by a number of perturbation techniques. Here the method of multiple time scales (MTS) is used. Accordingly the solution in terms of different time scales is expressed as

$$q(t;\varepsilon) = q_0(T_0,T_1) + \varepsilon q_1(T_0,T_1) + \ldots \tag{39}$$

where $T_0=t$ and $T_1=\varepsilon t$. The excitation in terms of T_0 and T_1 is expressed as

$$E(t)=\varepsilon K\cos(\omega_0 T_0+\sigma T_1) \tag{40}$$

Substituting Eqs(40) and (39) into Eq. (37) and equating the coefficient of ε^0 and ε^1 on both sides, we obtain

$$D_0^2 q_0+\omega_0^2 q_0=0 \tag{41}$$

$$D_0^2 q_1+\omega_0^2 q_1=-2D_0D_1q_0-\gamma q_0^3+k\cos(\omega_0 T_0+\sigma T_1) \tag{42}$$

The general solution of Eq. (41) can be written as

$$q_0=A(T_1)\exp(i\omega_0 T_0)+\bar{A}(T_1)\exp(-i\omega_0 T_0) \tag{43}$$

where $A(T_1)$ is an undetermined function at this point. Substituting Eqs. (43) in Eq. (42) and extracting secular terms which are coefficients of $e^{\pm i\omega_0 T_0}$ solvability equation will be determined as:

$$2i\omega_0 A'+3\gamma A^2\bar{A}-\frac{1}{2}k\exp(i\sigma T_1)=0 \tag{44}$$

Letting A in polar form

$$A=\frac{1}{2}a\exp(i\beta) \tag{45}$$

where a and β are real. Separating real and imaginary parts of derived equation, it yields

$$a'=\frac{1}{2}\frac{k}{\omega_0}\sin(\sigma T_1-\beta) \tag{46a}$$

$$a\beta'=\frac{3}{8}\frac{\gamma}{\omega_0}a^3-\frac{1}{2}\frac{k}{\omega_0}\cos(\sigma T_1-\beta) \tag{46b}$$

Term T_1 can be eliminated by transforming Eqs. (46) to an autonomous system [24] considering:

$$\theta=\sigma T_1-\beta \tag{47}$$

and substituting Eq. (47) in Eqs. (46) lead to:

$$a'=\frac{1}{2}\frac{k}{\omega_0}\sin(\theta) \tag{48a}$$

$$a\theta'=\sigma a-\frac{3}{8}\frac{\gamma}{\omega_0}a^3+\frac{1}{2}\frac{k}{\omega_0}\cos(\theta) \tag{48b}$$

The point which $a' = 0$ and $\theta' = 0$ corresponds to singular point of the system and shows the steady-state motion of system [38] . So, in steady-state condition it can be written:

$$0 = \frac{1}{2}\frac{k}{\omega_0}\sin(\theta) \tag{49a}$$

$$\sigma a - \frac{3}{8}\frac{\gamma}{\omega_0}a^3 = -\frac{1}{2}\frac{k}{\omega_0}\cos(\theta) \tag{49b}$$

Squaring and adding these equations, one may obtain the frequency response equation

$$\left(\sigma - \frac{3}{8}\frac{\gamma}{\omega_0}a^2\right)^2 a^2 = \frac{k^2}{4\omega_0^2} \tag{50}$$

Substituting Eq. (45) into Eq. (43) and substituting that result into Eq. (39), one may obtain the first approximation

$$q = a\cos(\omega_0 t + \beta) + O(\varepsilon) \tag{51}$$

Substituting Eqs. (47) and (38) into Eq. (50), the first approximation to the steady state solution is given by

$$q = a\cos(\omega_0 t + \varepsilon\sigma t - \theta) + O(\varepsilon) = a\cos(\Omega t - \theta) + O(\varepsilon) \tag{52}$$

it can be found the detuning parameter is as follow:

$$\sigma = \frac{3}{8}\frac{\gamma}{\omega_0}a^2 \pm \frac{k}{2\omega_0 a} \tag{52}$$

Fig. 5 shows the effects of k on the amplitude of the system with respect to detuning parameter σ. Fig. 6 demonstrates the effects of γ on the amplitude of the system with respect to detuning parameter σ.

5. NUMERICAL RESULTS

Figure 1 plot the nonlinear fundamental frequency ratio versus dimensionless amplitude curves for beam. Beam exhibit typical hardening behavior, i.e., the nonlinear frequency ratio increases as the vibration amplitude is increased. Fig. 2 shows how frequency ratios, μ, predicted by the non-classical beam theory change with the beam thickness (or *h/ℓ*). Figure 3 displays the phase plane diagrams (q versus $\dot{q}$) for beam. Figure 4 gives dimensionless vibration amplitude as a function of dimensionless time for beams

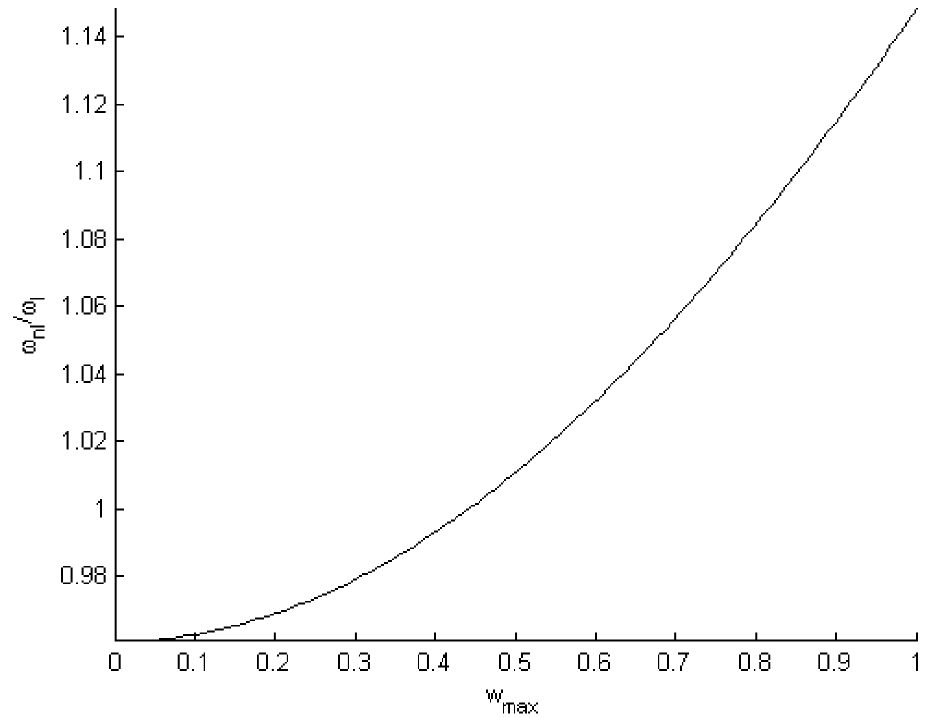

Fig. 1 Nonlinear frequency ratio versus dimensionless amplitude curves for beams

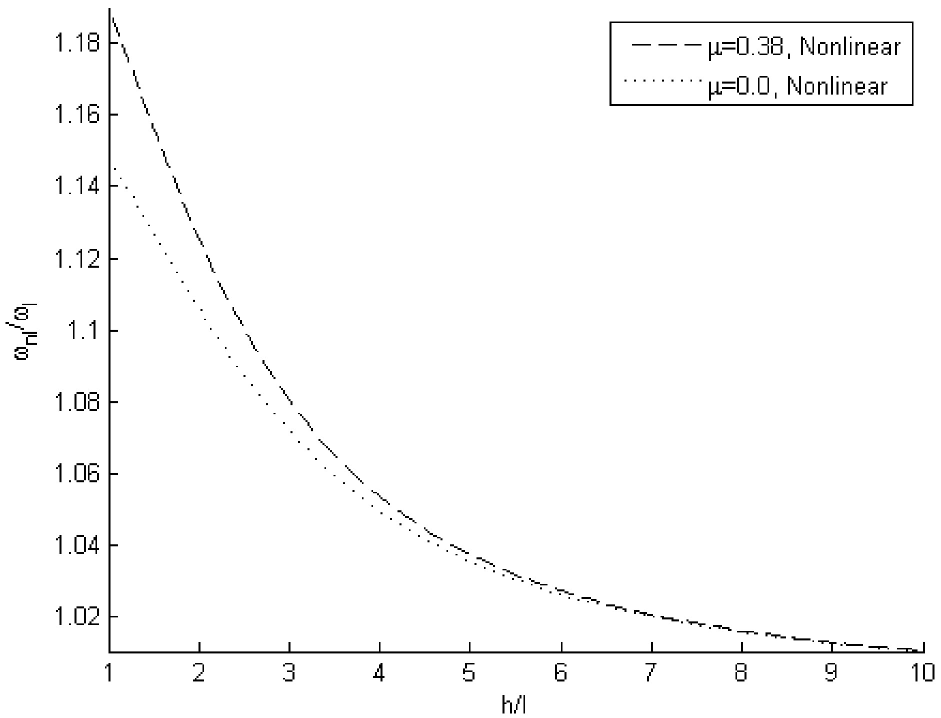

Fig. 2. The ratio of the non-classical frequency to the linear classical frequency as a function of *h/ℓ*.

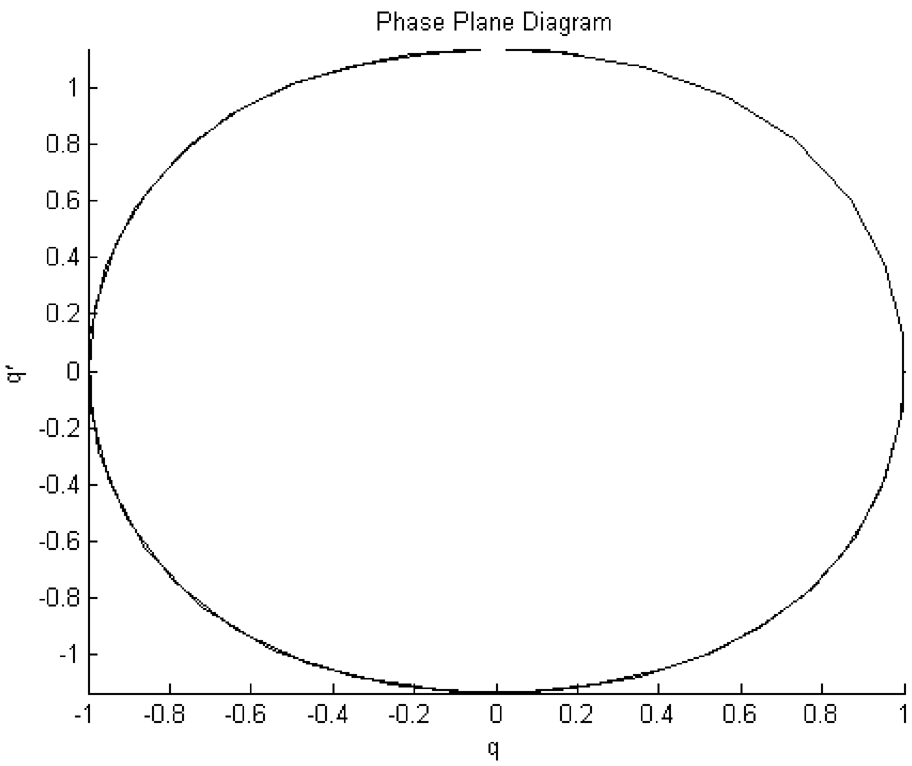

Fig. 3. Phase plane diagram for nonclassical microscale beam.

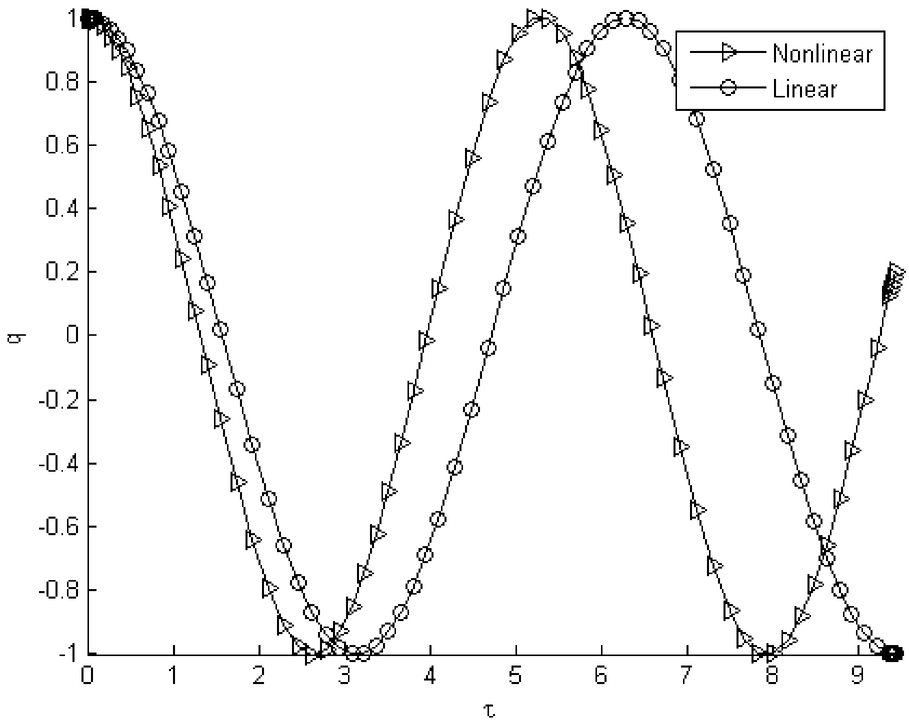

Fig. 4. Time history of dimensionless amplitudes for non-classical microscale beams

The results displayed in Fig. 2 are obtained from Eq. (35), for non-classical beam model. To illustrate the Poisson effect, two different values of Poisson's ratio, i.e., $\mu = 0$ and $\mu = 0.38$ are used. It is worth noting that, when h/ℓ is approximately equal to one, the size effect is remarkably visible.

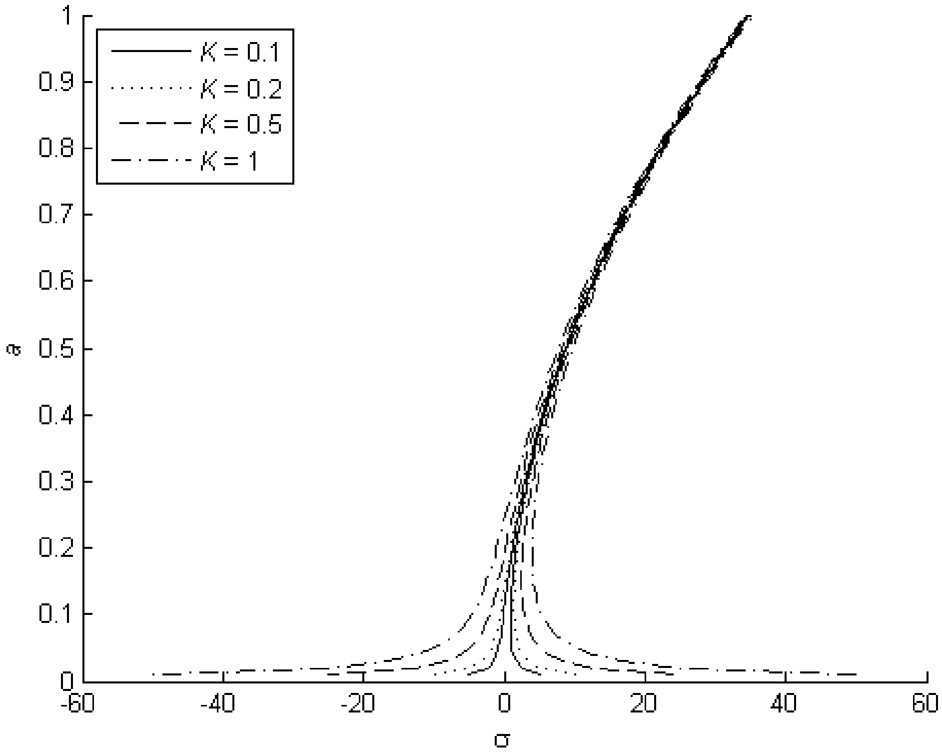

Fig 5. Effects of amplitude of excitation k for γ = 100 in primary resonance.

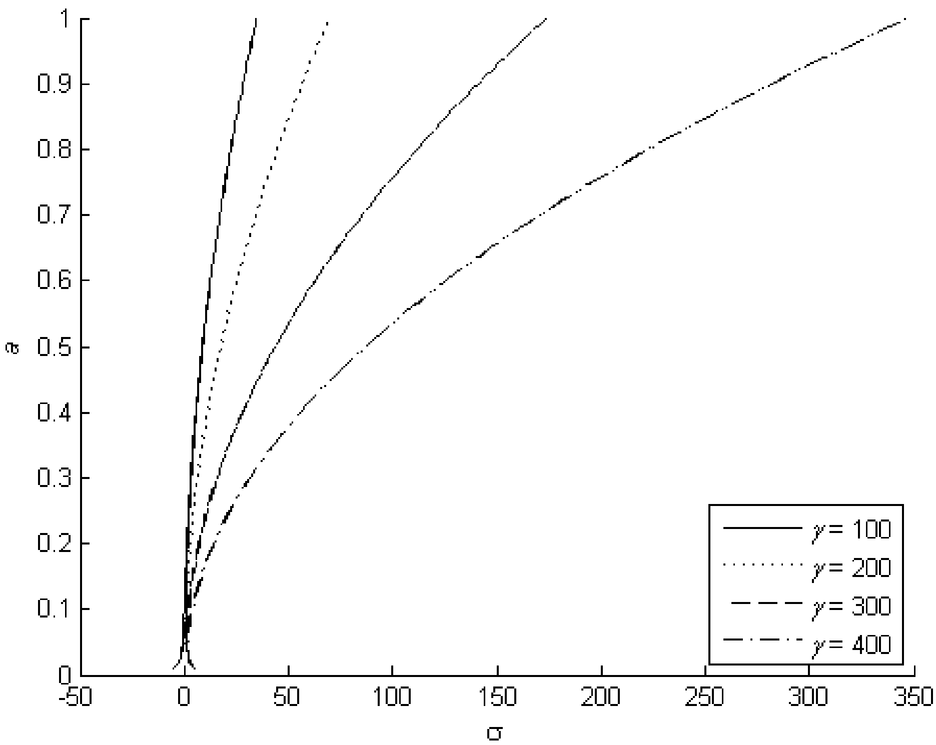

Fig 6. Effects of γ for k = 0.1 in primary resonance.

6. CONCLUSIONS

A nonlinear non-classical Euler–Bernoulli beam model with an energy formulation to study the free and forced vibration behavior of microscale beams on immovable ends has been developed. In the present nonlinear model, the nonlinearity associated with the internal material length scale constant considered. The analysis is performed within the context of non-classical continuum mechanics. For the free vibration of a microscale beam, it is found that the nonlinear frequencies are much higher than the linear ones. Therefore, compared with the linear non-classical beam model, the nonlinear non-classical model and its conclusions regarding vibration properties may be more reliable. The results obtained in this paper highlight the importance of considering nonlinearity and size effects in the proper design of microscale devices and systems such as biosensors, atomic force microscopes and MEMS. In the next section, the forced vibrations of the system were studied for the first time. First, the primary resonances of the system by using the MTS method were studied and the frequency-response equation of the system was presented and the effects of different parameters on the response of the system were investigated. Then non-resonant hard excitation case was studied and the frequency of free oscillation of the system and the effect of different parameters were investigated. In addition, in the final sections super-harmonic and sub-harmonic resonances were studied and in the both cases the frequency-response equations and the effect of different parameters on the response of the system were shown.

References

[1] M. Moghimi Zand, M.T. Ahmadian, Characterization of coupled-domain multi-layer microplates in pull-in phenomenon, International Journal of Mechanical Sciences 49 (2007) 1226–1237.

[2] C.W. Lim, L.H. He, Size-dependent nonlinear response of thin elastic films with nano-scale thickness, International Journal of Mechanical Sciences 46 (2004) 1715-1726.

[3] J. Pei, F. Tian, T. Thundat, Glucose biosensor based on the microcantilever, Analytical Chemistry 76 (2004) 292–297.

[4] M. Li, H.X. Tang, M.L. Roukes, Ultra-sensitive NEMS-based cantilevers for sensing, scanned probe and very high-frequency applications, Nature Nanotechnology 2 (2007) 114–120.

[5] N.A. Stelmashenko, M.G. Walls, L.M. Brown, Y.V. Milman, Microindentations on W and Mo oriented single crystals: an STM study, Acta Metallurgica et Materialia 41 (1993) 2855–2865.

[6] W.J. Poole, M.F. Ashby, N.A. Fleck, Micro-hardness of annealed and work-hardened copper polycrystals, Scripta Materialia 34 (1996) 559–564.

[7] S.K. Park, X.-L. Gao, Bernoulli–Euler beam model based on a modified couple stress theory, Journal of Micromechanics and Microengineering 16 (2006) 2355–2359.

[8] M. Asghari, M.T. Ahmadian, M.H. Kahrobaiyan, M. Rahaeifard, On the size-dependent behavior of functionally graded micro beams, Materials and Design 31 (2010) 2324–2329.

[9] L. Wang, Size-dependent vibration characteristics of microtubes conveying fluid, Journal of Fluids and Structures, in press. doi:10.1016/ j.jfluidstructs.2010.02.005.

[10] L. Wang, Dynamical behaviors of double-walled carbon nanotubes conveying fluid accounting for the role of small length scale, Computational

Materials Science 45 (2009) 584–588.
[11] N.A. Fleck, G.M. Muller, M.F. Ashby, J.W. Hutchinson, Strain gradient plasticity: theory and experiment, Acta Metallurgica et Materialia 42 (1994) 475–487.
[12] Q. Ma, D.R. Clarke, Size dependent hardness of silver single crystals, Journal of Materials Research 10 (1995) 853–863.
[13] J.S. Stolken, A.G. Evans, Microbend test method for measuring the plasticity length scale, Acta Materialia 46 (1998) 5109–5115.
[14] A.C.M. Chong, D.C.C. Lam, Strain gradient plasticity effect in indentation hardness of polymers, Journal of Materials Research 14 (1999) 4103–4110.
[15] D.C.C. Lam, F. Yang, A.C.M. Chong, J. Wang, P. Tong, Experiments and theory in strain gradient elasticity, Journal of the Mechanics and Physics of Solids
51 (2003) 1477–1508.
[16] A.W. McFarland, J.S. Colton, Role of material microstructure in plate stiffness with relevance to microcantilever sensors, Journal of Micromechanics and Microengineering 15 (2005) 1060–1067.
[17] R.D. Mindlin, Micro-structure in linear elasticity, Archive for Rational Mechanics and Analysis 16 (1964) 51–78.
[18] R.D. Mindlin, H.F. Tiersten, Effects of couple-stresses in linear elasticity, Archive for Rational Mechanics and Analysis 11 (1962) 415–448.
[19] R.A. Toupin, Elastic materials with couple-stresses, Archive for Rational Mechanics and Analysis 11 (1962) 385–414.
[20] F. Yang, A.C.M. Chong, D.C.C. Lam, P. Tong, Couple stress based strain gradient theory for elasticity, International Journal of Solids and Structures 39 (2002) 2731–2743.
[21] S.L. Kong, S.J. Zhou, Z.F. Nie, K. Wang, The size-dependent natural frequency of Bernoulli–Euler micro-beams, International Journal of Engineering Science 46 (2008) 427–437.
[22] H. Sadeghian, G. Rezazadeh, P.M. Osterberg, Application of the generalized differential quadrature method to the study of pull-In phenomena of MEMS switches, Journal of Microelectromechanical Systems 16 (2007) 1334–1340.
[23] C.W. Bert, M. Malik, Differential quadrature method in computational mechanics: a review, Applied Mechanics Reviews 49 (1996) 1–27.
[24] A.H. Nayfeh, D.T. Mook, Nonlinear Oscillations, John Wiley, New York, 1979.
[25] M.A. Foda, On non-linear free vibrations of a beam with pinned ends, Journal of King Saud University 7 (1995) 93–107.
[26] Byrd, P.F., Friedman, M.D., 1971, handbook of Elliptic Integrals for Engineers and Scientis, Berlin.
[27] Zhou SJ, Li ZQ. Length scales in the static and dynamic torsion of a circular cylindrical micro-bar. J Shandong Univ Technol 2001;31(5):401–7.
[28] Kang X, Xi XF. Size effect on the dynamic characteristic of a micro beam based on Cosserat theory. J Mech Strength 2007;29(1):1–4.